



Phase transformation in the Niobium Hydrogen system: Effects of elasto-plastic deformations on phase stability predicted by a thermodynamic model

Alexander Dyck^a, Thomas Böhlke^a, Astrid Pundt^b, Stefan Wagner^{b,*}

^a Institute of Engineering Mechanics - Chair for Continuum Mechanics, Karlsruhe Institute of Technology (KIT), Kaiserstraße 10, 76131 Karlsruhe, Germany

^b Institute for Applied Materials – Materials Science and Engineering, Karlsruhe Institute of Technology (KIT), Engelbert-Arnold-Straße 4, 76131 Karlsruhe, Germany

ARTICLE INFO

Keywords:

Metal-hydrogen system
Thin film
Elasto-plastic deformation
Equilibrium concentrations
Critical temperature

ABSTRACT

Constraint conditions and elasto-plastic deformation alter phase stabilities of metal-hydrogen systems. Experiments on niobium-hydrogen thin films reveal, that elastically deforming films suppress hydride formation at 300 K, while elasto-plastically deforming films can form a hydride phase. Building upon a thermodynamic model studying the coupling of elastic deformations, constraint conditions and phase separation, elasto-plastic deformations are incorporated to investigate hydride formation. The stress state for each constraint condition for both elastically and elasto-plastically deforming Nb is specified. The monotony of the resulting chemical potential reveals hydride formation to be possible in elasto-plastically deforming niobium-hydrogen films, while it is suppressed by large stresses in elastically deforming films. Critical temperatures of hydride formation and miscibility gaps for both elastically and plastically deforming niobium are computed. The critical temperature is way below 300 K in elastically deforming films, while it is close to that of a stress free system in strongly elasto-plastically deforming films.

Mechanical stresses and constraint conditions can alter the phase stability in alloy systems undergoing structural phase transitions. In nano-scale systems, constraint conditions can, e.g., result from the surfactant shell or the scaffold stabilizing clusters, from thin film adherence to a rigid substrate, but also from the coherency of the phase interfaces [1–8]. The constraints are related to the hydrostatic pressure applied by a surfactant shell, or to the lattice misfit between film and substrate and between different thermodynamic phases of a system [2,3,9–12]. The effects of mechanical stresses and strains on phase stabilities can easily be studied for metal-hydrogen systems, where the hydrogen concentration in the metal can be adjusted by simply changing the hydrogens' chemical potential in gas phase or electrochemical charging experiments [1,2,4,9,10,13–18].

In a recent publication [21], we investigated the palladium-hydrogen (Pd-H) system and the influence of elastic deformations and constraint conditions on its thermodynamic properties from a theoretical point of view. It was shown, that at room temperature, in a 2D constrained system mimicking the conditions of thin films adhered to a rigid substrate, phase separation in α and α' (β)-phase is possible for the Pd-H system [21]. However, in experimental studies on the niobium-

hydrogen (Nb-H) system, it was shown that this observation does not hold for very thin films, see e.g. [10,20,22]. In these works, epitaxial thin Nb films with varying thicknesses, e.g., 5 nm, 8 nm and 40 nm, were deposited on sapphire substrates and loaded with hydrogen. In-situ scanning tunneling microscope (STM) and substrate curvature measurements were conducted, the latter giving access to the in-plane stress state of the films by means of Stoney's formula [23]. Results of these experimental investigations are summarized in Fig. 1, where STM images are shown in a) and b) while the stresses are shown in c). In the 40 nm-film, the formation of hydride precipitates is evident, accompanied by strong elasto-plastic deformations of the film, where the relation between stresses and hydrogen concentration shows two distinct regimes with different slopes. However, in the 5 and 8 nm-films, hydride formation is suppressed. Instead, a Nb-H solid solution with concentrations up to $c_H = 1.0 \text{ H/Nb}$ forms. This is evident by the STM measurements of an 8 nm-film, shown in the STM difference image in Fig. 1b, where only traces of dislocations are visible as yellow lines. Further, this is supported by in-situ X-Ray diffraction experiments [10,19,20]. While the hydrogen absorption in the 5 nm film is accompanied by purely elastic deformations [20], in the 8 nm-film some misfit dislocations form be-

* Corresponding author.

E-mail address: stefan.wagner3@kit.edu (S. Wagner).

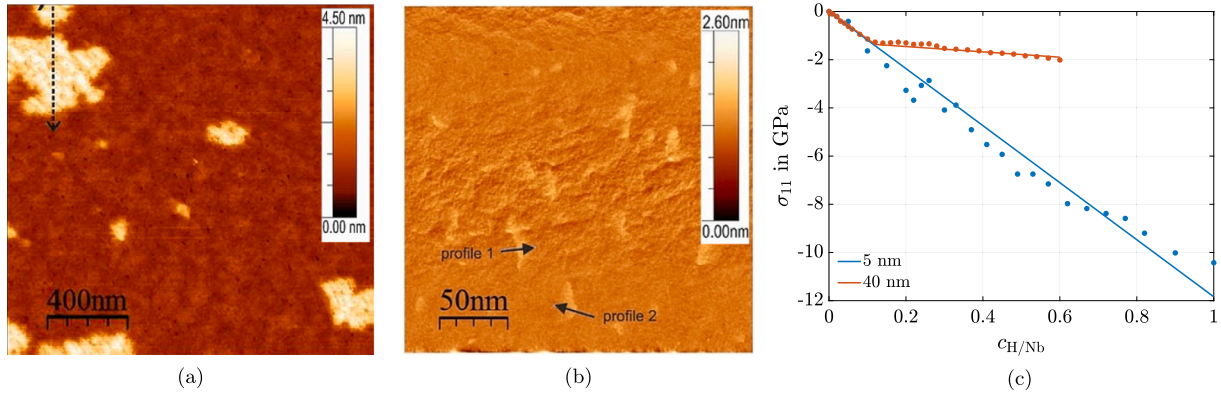


Fig. 1. a) STM surface topography image of a 40 nm epitaxial Nb thin film adhered to sapphire substrate upon hydrogen loading at $p_{\text{H}_2} = 1 \times 10^{-6}$ mbar and 293 K. The figure reveals the formation of hydride precipitates by the presence of elevated yellow areas at these conditions. b) STM surface topography difference image of an 8 nm Niobium film after cyclic hydrogen loading at even higher pressure of $p_{\text{H}_2} = 8 \times 10^{-6}$ mbar at 293 K. During loading no hydride formation like in (a) was observed, but some misfit dislocations have emerged between film and substrate, resulting in step lines at the film surface. Both figures are reproduced with permission from Ref. [19]. c) Experimentally determined stresses in 5 and 40 nm thin Nb films using the substrate curvature measurement (dotted) [20] and piecewise linear fits to the data (solid lines) using Eq. (11). (For interpretation of the colors in the figure(s), the reader is referred to the web version of this article.)

tween film and substrate. These observations can not be predicted using the purely linear-elastic model outlined in [21]. Hence, in this work, we incorporate elasto-plastic deformations into the chemo-mechanically coupled thermodynamic model to address hydride formation in elasto-plastically deforming Nb films.

In the following, the thermodynamic model is summarized. The independent variables are the dimensionless hydrogen concentration c_{H} in H/Nb, which results from the total concentration c in moles per volume divided by the maximum concentration c_{max} as determined by the atomic structure. In addition, temperature θ , the total strain $\underline{\epsilon}$ and internal variables $\underline{\alpha} = [\epsilon_{\text{p}}, \epsilon_{\text{pe}}]$, which are the plastic strains ϵ_{p} and the scalar equivalent plastic strains ϵ_{pe} , are introduced as independent variables. These are collected in the set $\Lambda = [c_{\text{H}}, \theta, \underline{\epsilon}, \underline{\alpha}]$. The thermodynamics of the metal-hydrogen system are governed by a free energy density $\psi(\Lambda)$, which is additively decomposed into a chemical part $\psi_{\text{c}}(c_{\text{H}}, \theta)$ and an elastic part $\psi_{\text{e}}(\underline{\epsilon}_{\text{e}})$ [24]

$$\psi(\Lambda) = \psi_{\text{c}}(c_{\text{H}}, \theta) + \psi_{\text{e}}(\underline{\epsilon}_{\text{e}}). \quad (1)$$

The chemical part of the free energy is independent of elastic strains $\underline{\epsilon}_{\text{e}}$, which are given by

$$\underline{\epsilon}_{\text{e}} = \underline{\epsilon} - \underline{\epsilon}_{\text{c}} - \underline{\epsilon}_{\text{p}}, \quad (2)$$

while the elastic part depends solely on the elastic strains. Chemical strains $\underline{\epsilon}_{\text{c}}$ arise due to the presence of hydrogen atoms in interstitial lattice sites and are given by

$$\underline{\epsilon}_{\text{c}} = \eta_{\text{H}} c_{\text{H}} \mathbf{I}, \quad (3)$$

where η_{H} is a linear lattice expansion coefficient and \mathbf{I} the identity tensor. The two parts of the free energy density are given by [21]

$$\begin{aligned} \psi_{\text{c}} = & \mu_0 c_{\text{H}} c_{\text{max}} + R\theta c_{\text{max}} \left(-r \ln \left(\frac{r}{r - c_{\text{H}}} \right) + c_{\text{H}} \ln \left(\frac{c_{\text{H}}}{r - c_{\text{H}}} \right) \right) \\ & - \frac{c_{\text{max}}}{2} E_{\text{HH}} c_{\text{H}}^2, \end{aligned} \quad (4)$$

$$\psi_{\text{e}} = \frac{1}{2} \underline{\epsilon}_{\text{e}} \cdot \mathbb{C} [\underline{\epsilon}_{\text{e}}].$$

The chemical part takes into account the mixture entropy of interstitial hydrogen atoms in the metal lattice as well as H-H interactions expressed via E_{HH} . The parameter r is the maximum hydrogen concentration from a H-H interaction perspective, μ_0 is a standard reference potential and R is the universal gas constant. The elastic part is quadratic in the elastic strains with stiffness tensor \mathbb{C} . In comparison to our previous work [21], the elastic part of the free energy incorporates

plastic strains. It is pointed out, that no term accounting for energy storage due to plasticity-induced defect accumulation is considered in the free energy density. This implies, that the entire plastic power is dissipated into heat. Since the dimension of the thin film and the time-scale of heat conduction are small compared to the time-scale of diffusive processes, this is not investigated further. However, it is pointed out, that a detailed discussion of formulations for energy storage due to defect accumulation can be found in, e.g., [25]. Following standard reasoning, see, e.g., [24], the potential relations linking the chemical potential μ_{H} and the mechanical stresses σ to the free energy density are assumed to be valid in the thermodynamic equilibrium and also during inelastic deformations. They result in [21,24]

$$\mu_{\text{H}} = \frac{\partial \psi}{\partial c_{\text{H}}} \frac{1}{c_{\text{max}}} = \mu_0 + R\theta \ln \left(\frac{c_{\text{H}}}{r - c_{\text{H}}} \right) - E_{\text{HH}} c_{\text{H}} - \eta_{\text{H}} v_0 \text{tr}(\sigma), \quad (5)$$

$$\sigma = \frac{\partial \psi}{\partial \underline{\epsilon}} = \mathbb{C} [\underline{\epsilon} - \underline{\epsilon}_{\text{c}} - \underline{\epsilon}_{\text{p}}].$$

Several assumptions are introduced, in order to arrive at a comparably simple theory, still capturing the essence of the experimentally observed behavior outlined above. These are:

- Nb is assumed to be elastically and plastically isotropic. This implies, that the stiffness tensor \mathbb{C} is fully characterized by Young's Modulus E and Poisson's ratio ν , while the plastic behavior can be described by an isotropic von Mises plasticity theory [26].
- Based on the measured stresses shown in Fig. 1 c), a linear hardening behavior is assumed. The yield strength is $\sigma_{\text{Y}}(\epsilon_{\text{pe}}) = \sigma_{\text{Y}0} + h\epsilon_{\text{pe}}$, with initial yield strength $\sigma_{\text{Y}0}$ and hardening modulus h .
- All independent variables, as well as all material parameters are assumed to be homogeneous, i.e. no fluctuations of concentrations, metal composition or material properties are present. This implies, that all parts of the metal will undergo plastic deformation as well as phase separation simultaneously when the concentration is increased. In previous studies on metal-hydrogen thin films, see e.g. [1,27], it has been shown, that heterogeneities in material properties and concentration fluctuations lead to sequential plastic deformations and thus to sloped plateaus in the two-phase region, where the conventional Gibbs phase rule [28], assuming constant chemical potential in the two-phase region, cannot be applied. This is out of the scope of the model presented in this work. Our model rather leads to an effective expression for the stresses and the chemical potential and, when the monotony of the chemical potential is studied, to effective critical temperatures as well as spinodal and binodal concentrations for a thin film metal-hydrogen system.

The evolution of the internal variables $\underline{\alpha}$ is given by a rate-independent von Mises plasticity theory [26]. The yield function, that limits the elastic range, is

$$\varphi(\sigma, \varepsilon_{pe}) = \sqrt{\frac{3}{2}} \|\sigma'\| - \sigma_Y(\varepsilon_{pe}) \leq 0, \quad (6)$$

where $\sigma' = \sigma - \text{tr}(\sigma)/3$ is the deviatoric part, while $\text{tr}(\sigma)/3$ is the spherical part of the stress tensor. The internal variables evolve according to

$$\dot{\varepsilon}_p = \gamma \frac{\sigma'}{\|\sigma'\|} = \gamma N, \quad \dot{\varepsilon}_{pe} = \sqrt{\frac{2}{3}} \gamma, \quad (7)$$

with the consistency parameter $\gamma \geq 0$. It evolves during plastic deformation when the yield condition $\varphi = 0$ and the loading condition $\sigma \cdot \dot{\varepsilon} > 0$ are fulfilled and ensures, that the consistency condition $\dot{\varphi} = 0$ is not violated during plastic deformation. The thermodynamic consistency of similar models has been detailed, e.g., in [24,29,30] and is not further discussed here.

Using the outlined thermodynamic model, hydride formation can be studied in elasto-plastically deforming metal hydrogen systems. Hydride formation is possible, when μ_H is a non-monotonous function of c_H [1]. The monotony of μ_H can be investigated by differentiating with respect to the concentration and studying the sign of the resulting function. The differentiation results in

$$c_{\max} \frac{\partial^2 \psi}{\partial c_H^2} = \frac{\partial \mu_H}{\partial c_H} = \frac{R\theta r}{rc_H - c_H^2} - v_0 \eta_H t - E_{HH}, \quad (8)$$

where

$$t = \frac{\partial \text{tr}(\sigma)}{\partial c_H}. \quad (9)$$

Thus, for given θ and E_{HH} , the resulting stresses either suppress or allow hydride formation to occur. As long as there exists a spinodal composition $c_H^{\text{sp}} \in [0, r]$, for which

$$\left. \frac{\partial \mu_H}{\partial c_H} \right|_{c_H^{\text{sp}}} = 0 \quad (10)$$

holds, phase separation is possible. Equilibrium concentrations of the phases with the maximum solubility c_{α}^{\max} of the solid solution phase and the minimum concentration $c_{\alpha'(\beta)}^{\min}$ of the hydride phase can be deduced via Maxwell constructions of the chemical potential given in Eq. (5)-(1). Additionally, by rearranging Eq. (8), a critical temperature θ_{crit} can be determined, above which no phase separation is possible for given E_{HH} and t [21]. In the following, mechanical stresses are derived as a function of the mean (homogeneous) hydrogen concentration c_H for both elastically and elasto-plastically deforming Nb films under different constraint conditions. With these results, phase separation and its suppression in the NbH-system is studied and compared to experimental results.

Niobium absorbs hydrogen on tetrahedral interstitial lattice sites. Targeting the free Nb-H bulk system as a reference [31], niobium hydride phases form below the critical temperature $\theta_{\text{crit}} = 444$ K. At room temperature, the solid solution limit of the body-centered cubic (bcc) α -phase is $c_{\alpha}^{\max} = 0.06$ H/Nb, which is in equilibrium with the face-centered orthorhombic β -phase of $c_{\beta}^{\min} = 0.72$ H/Nb composition at intermediate global H concentrations. Above 360 K, an α' -hydride phase with bcc structure exists. For simplicity, in the present model we focus on the iso-structural α - and α' -phases.

In order to study hydride formation, the occurring stresses have to be determined as a function of hydrogen concentration [21]. As outlined above, elasto-plastic deformations in Nb thin-films under hydrogen loading have been demonstrated via substrate curvature measurements, yielding the σ_{11} component, see e.g. [20] and Fig. 1 c). In the 5 nm Nb-H film, the in-plane stresses σ_{11} are linear in hydrogen concentration c_H in the concentration range of interest up to $c_H = 0.7$ H/Nb, revealing

Table 1

Piecewise linear fit of the experimentally determined stresses by means of Eq. (11) for both 5 nm and 40 nm films.

Film height	m	d	\hat{c}_H	R^2
5 nm	-11.84 GPa	0 GPa		0.9625
40 nm (elastic domain)	-11.37 GPa	0 GPa		0.9893
40 nm (plastic domain)	-1.11 GPa	-1.23 GPa	0.12 H/Nb	0.8405

the absence of plastic deformation. However, in the 40 nm Nb-H film, at $c_H = \hat{c}_H = 0.12$ H/Nb, the slope of $\sigma_{11}(c_H)$ changes strongly. This is interpreted as the onset of plastic deformation [10,19]. For $c_H \geq \hat{c}_H$, plastic deformations occur and lower the stresses drastically compared to the purely elastic case. Both experimentally determined curves are linear (5 nm) or piecewise linear (40 nm) in c_H . For the following considerations, these measurements are approximated by

$$\sigma_{11}(c_H) = m c_H + d. \quad (11)$$

Results, including R^2 values of the fit functions, are summarized in Table 1. In the linear elastic regime, both 5 nm and 40 nm films have a similar slope of $m_e \approx -11$ GPa, resembling the linear elastic limit [20]. In the plastic domain of the 40 nm film, the slope changes drastically to $m_p \approx -1.1$ GPa. We emphasize that, in general, the plasticity parameters such as σ_{Y0} and h , and thus \hat{c}_H and m_p will be functions of the Nb film thickness, grain structure and crystallographic texture [2]. Thus, for varying processing conditions of the films, different slopes m_p as well as different concentrations \hat{c}_H , at which plastic deformation in the film initiates, will result. In the following, an elasto-plastically deforming NbH system will be studied and subjected to various constraint conditions, cf. Fig. 2 and [21]. Emphasis is put on the 2D constraint, cf. Fig. 2 c), as this constraint is equivalent to a Nb thin film adhered to a rigid substrate. For increasing dimensionality of the constraints, the expansion of the metal is increasingly restricted and the build up in stress rises. This results in drastically differing stress states in the elastic regime, i.e. differing slopes m_e for each constraint. Following [21], the slopes m_e in the elastic regime are given for each constraint by

$$\begin{aligned} m_e^{0D} = 0 &= \frac{\sigma_{11,e}^{0D}}{c_H} = \frac{\sigma_{22,e}^{0D}}{c_H} = \frac{\sigma_{33,e}^{0D}}{c_H}, \\ m_e^{1D} &= -\eta_H E = \frac{\sigma_{11,e}^{1D}}{c_H}, \quad \frac{\sigma_{22,e}^{1D}}{c_H} = \frac{\sigma_{33,e}^{1D}}{c_H} = 0, \\ m_e^{2D} &= \frac{\eta_H E}{\nu - 1} = \frac{\sigma_{11,e}^{2D}}{c_H} = \frac{\sigma_{22,e}^{2D}}{c_H}, \quad \frac{\sigma_{33,e}^{2D}}{c_H} = 0, \\ m_e^{3D} &= \frac{\eta_H E}{2\nu - 1} = \frac{\sigma_{11,e}^{3D}}{c_H} = \frac{\sigma_{22,e}^{3D}}{c_H} = \frac{\sigma_{33,e}^{3D}}{c_H}. \end{aligned} \quad (12)$$

As the measured in-plane stresses for the 40 nm thin film shown in Fig. 1 c) indicate $m_e^{2D} = -11$ GPa as well as $\hat{c}_H^{2D} = 0.12$ H/Nb, the elasticity parameters are chosen to be $E = 132$ GPa and $\nu = 0.3$. Inserting the identified elasticity parameters into the stresses for the 1D constrained system results in $\hat{c}_H^{1D} = 0.18$ H/Nb. In the 3D case no plastic deformation occurs, as the stress state is spherical and only deviatoric stresses lead to plastic deformations according to the chosen von Mises yield criterion. In the plastic regime, the stresses increase, again, linear with c_H , due to the assumed linear hardening, see Table 1. For generalization we investigate different magnitudes of slopes m_p for each constraint in the following to study the influence of the hardening behavior on the thermodynamics of the system. The stresses in the plastic regime are thus expressed as

$$\begin{aligned} \sigma_{11}^{1D,p} &= m_p^{1D} c_H, \\ \sigma_{11}^{2D,p} &= \sigma_{22}^{2D,p} = m_p^{2D} c_H. \end{aligned} \quad (13)$$

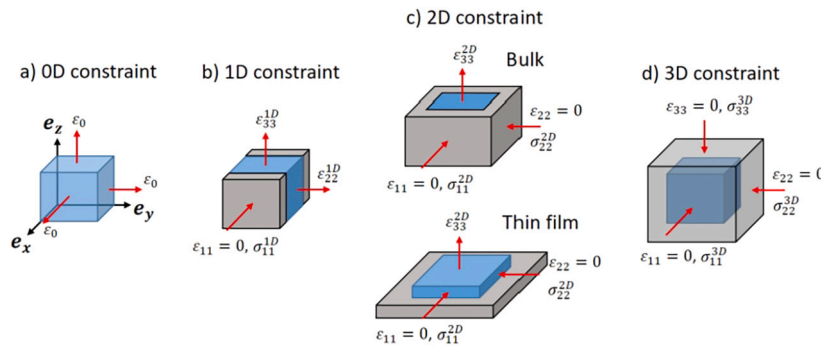


Fig. 2. Metal-hydrogen systems with different J/mol constraint conditions. The grey frames visually indicate the directions of the constraint condition. Expansion of the sample cube is a) possible in all directions (0D constraint), b) suppressed in e_x -direction, c) suppressed in e_x - and e_y -direction, and d) entirely suppressed by placing the cube in a rigid shell. The 2D constraint condition is equivalent to the 2D elastic constraint of an adhered thin film with thickness much smaller than the lateral dimensions. In this case, the lateral expansion is suppressed by the film's adherence to a rigid substrate, and the film can only expand in e_z -direction [32]. Actually, the lateral expansion of a 1 cm wide and 40 nm thick Nb film resulting at the top of the film is of the order of 10 nm [33].

Table 2

Model parameters used in this work. Chemical parameters are taken from Ref. [19], mechanical parameters are chosen in this work.

R	θ	v_0	r	E_{HH}	η_{H}	E	ν
8.3145 J/mol	300 K	$9.71 \times 10^{-6} \text{ m}^3/\text{mol}$	0.67	20.2 kJ/mol	0.058	132 GPa	0.3
m_{c}^{1D}	m_{c}^{2D}	m_{c}^{3D}	m_{p}^{1D}	m_{p}^{2D}			
-7.6 GPa	-11 GPa	-19.1 GPa	[0, -1, ..., -7.6] GPa	[0, -1, ..., -11] GPa			

Thereby, both values m_{p}^{1D} and m_{p}^{2D} are limited by a vanishing slope, i.e. no hardening, and the respective elastic slope, implying $m_{\text{p}}^{\text{1D}} \in [0, m_{\text{c}}^{\text{1D}}]$ and $m_{\text{p}}^{\text{2D}} \in [0, m_{\text{c}}^{\text{2D}}]$. The derivative of trace of the stress state, introduced in Eq. (9), can now be computed via $t^{\text{XD}} = \sum_i m_i^{\text{XD}}$. We want to point out, that a computation of each stress component during elasto-plastic deformations as a function of c_{H} is possible in a semi-analytical way using a Computer-Algebra-System, when hardening modulus and initial yield strength are known. This procedure is detailed in the supplemental information of this article for a 2D constrained system.

Based on the resulting stress state as a function of hydrogen concentration c_{H} , i.e. the slopes in the elastic and plastic regime, the chemical potential given in Eq. (5)-(1), as well as equilibrium and spinodal concentrations of thin Nb films of varying thickness and under varying constraint conditions are studied. In addition, the critical temperatures of hydride formation according to Eq. (8) are calculated. The necessary chemical material parameters have been adapted from Ref. [19]. All chosen parameters are summarized in Table 2.

In order to verify the model predictions, we start with a direct comparison of the experimental results shown in Fig. 1 to the model predictions of a 2D constrained system. To this end, a temperature of $\theta = 300 \text{ K}$ is chosen and the chemical potential μ_{H} for purely elastic deformation (dotted yellow curve), mimicking a 5 nm film, and elasto-plastic deformation (solid yellow curve), mimicking a 40 nm film, are depicted in Fig. 3 a). The slope in the plastic regime is taken from Table 1. As outlined above, elastically deforming Nb thin films suppress phase separation at room temperature. This is reproduced by the derived model, as indicated by the monotonous increase of the chemical potential with respect to the overall hydrogen concentration in the 2D constrained system. This shows, that occurring stresses suppress phase separation at room temperature, in contrast to the 2D constrained PdH system studied in [21]. This different behavior results mainly from the lower hydrogen-hydrogen interaction strength E_{HH} in Nb-H compared to the Pd-H system, where $E_{\text{HH}} = 36.8 \text{ kJ/mol}$. The stability of the hydride phase is governed by the interplay of the stabilizing E_{HH} and the destabilizing contribution of $\eta_{\text{H}}v_0\text{tr}(\sigma)$, see Eq. (5). However, as plastic deformations drastically reduce occurring mechanical stresses,

a 40 nm thin film with a slope of $m_{\text{p}}^{\text{2D}} = -1.1 \text{ GPa}$ shows phase separation at room temperature. The proposed model confirms this finding, as the related chemical potential is a non-monotonous function of the concentration at room temperature in the 2D constrained case with plastic deformation. For the presented 5 nm film, however, stress relaxes too little to enable hydride formation. In addition to the occurrence of phase separation, the outlined model allows to compute both equilibrium concentrations for α - and hydride-phase as well as spinodal concentrations c_{H}^{sp} as a function of temperature, cf. Eq. (10). Equilibrium concentrations follow from a Maxwell construction using the known stress state. Results of this investigation are depicted in Fig. 3 b) for both 5 nm and 40 nm films, again using $m_{\text{p}}^{\text{2D}} = -1.1 \text{ GPa}$, in addition to a stress free system. Obviously, the occurrence of plastic deformations drastically increases the miscibility gap as well as the spinodal concentrations and the critical temperature θ_{crit} for hydride formation. In fact, the predicted critical temperature for the 40 nm film is only slightly lower compared to the stress free system, as occurring stresses are strongly reduced by plastic deformations. In the case of elastically deforming Nb with 2D constraint such as the 5 nm film, on the contrary, the critical temperature for hydride formation is about 160 K. As a final note it is pointed out that Eq. (10) is discontinuous at $c_{\text{H}} = \hat{c}_{\text{H}}$, as the slope in the stresses changes discontinuously. This implies, that for concentrations around the onset of plastic deformations the predictions of the spinodal concentration are to be considered inaccurate, as this behavior is obviously non-physical. However, the predicted equilibrium concentration for the α -phase at room temperature is $c_{\text{H}} \approx 0.12 \text{ H/Nb}$, i.e. at the onset of plastic deformations, which is in agreement with the experimental observations made in Ref. [19].

To show the capabilities of the presented model, we now study the influence of a variation in the plastic slope m_{p} on hydride formation for different constraint conditions, related to the actual microstructural conditions of a metal-hydrogen system. To illustrate the effect of this change, the critical temperature θ_{crit} is computed for each constraint condition for both purely elastically deforming and elasto-plastically deforming Nb, where the plastic slope is chosen to be in the interval given in Table 2. The results are depicted in Fig. 4. Apparently, the critical temperature of hydride formation changes linearly with the plastic

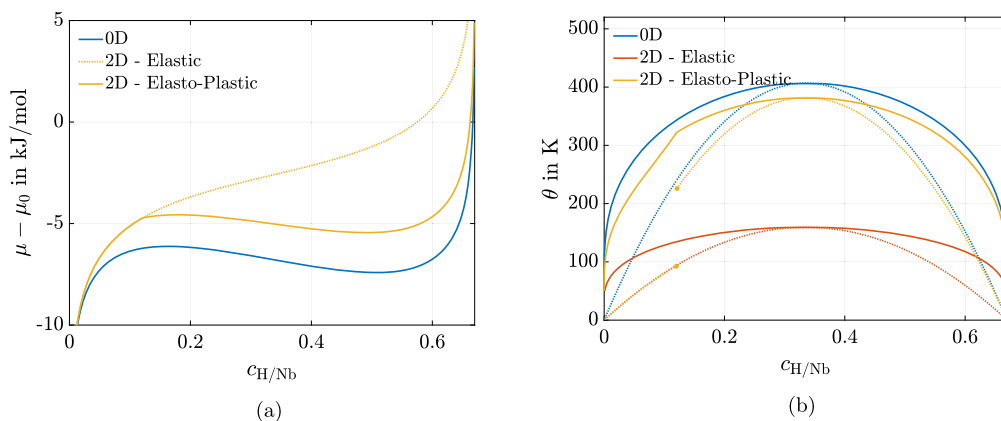


Fig. 3. a) Chemical potential of a linear elastic 5 nm and an elasto-plastically 40 nm deforming Nb-H film at $\theta = 300$ K using the model and stress states identified in Table 1. b) Spinodal and equilibrium concentrations of α - and hydride-phase for both films as a function of temperature. As the derivative of the chemical potential is non-continuous at $c_H = \hat{c}_H^{XD}$ for the 40 nm film, a jump is predicted in the spinodal concentrations. This is also visible in the equilibrium concentration curve for the elasto-plastically deforming Nb. The critical temperatures of hydride formation strongly differ for both films, enabling hydride formation at room temperature in the plastically deforming 40 nm film, while it is suppressed in the elastically deforming 5 nm film.

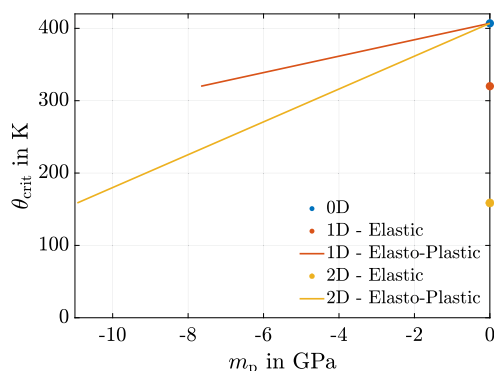


Fig. 4. Critical temperatures θ_{crit} for different constraints for elastically and elasto-plastically deforming Nb for different slopes m_p . In the 3D constrained system no hydride formation is possible due to the large stresses.

slope m_p for both 1D and 2D constrained systems, but with significantly larger slope for the 2D constraint. For vanishing slopes $m_p = 0$, the critical temperature of each film coincides with an unconstrained system, while at maximum slope, i.e. a slope identical to the elastic slope, the critical temperature is identical to the elastically deforming Nb. In the 3D constrained system, Nb-hydride formation is suppressed irrespective of temperature. We want to point out, that $\theta_{crit}^{0D} = 407$ K differs from the bulk value of 444 K. This is due to the parameter E_{HH} , which differs in miniaturized Nb-H systems from the bulk value [19].

To conclude this work, the main results are summarized as follows:

- A thermodynamic framework for elasto-plastically deforming metal-hydrogen systems is presented and compared with experimental results on Nb thin films under hydrogen loading.
- If Nb-films deform purely elastic upon hydrogen loading, the occurring stresses lead to a monotonically increasing chemical potential at room temperature as a function of the total hydrogen concentration. This implies, that no phase separation occurs upon hydrogen loading. This is in agreement with experiments on 5 nm Nb-H films.
- If Nb-films strongly deform elasto-plastic upon hydrogen loading, occurring stresses are drastically reduced and phase separation is possible at room temperature, indicated by a non-monotonous chemical potential predicted by the model. Again, the model predictions match experimental evidence of phase-separation in 40 nm films.
- The derived model allows to compute both spinodal and equilibrium concentrations for α - and hydride-phase. The equilibrium

concentration for the α -phase predicted by the model is in agreement with experimental observations.

- In general, the specific model parameters for plastic deformation such as the yield strength and the hardening modulus will be a function of the Nb film thickness. This can drastically change critical temperatures and widths of the miscibility gaps.
- In general, in metal-hydrogen systems hydride formation under different constraint conditions depends on the interplay of the attractive H-H interaction, evolving stresses and stress relaxation.

CRediT authorship contribution statement

Alexander Dyck: Writing – original draft, Visualization, Methodology, Investigation, Formal analysis, Conceptualization. **Thomas Böhlke:** Writing – review & editing, Supervision, Resources. **Astrid Pundt:** Writing – review & editing, Resources, Funding acquisition. **Stefan Wagner:** Writing – original draft, Validation, Methodology, Formal analysis, Conceptualization.

Declaration of competing interest

The authors declare that they have no known competing financial interests or personal relationships that could have appeared to influence the work reported in this paper.

Appendix. Supplementary material

Supplementary material related to this article can be found online at <https://doi.org/10.1016/j.scriptamat.2024.116209>.

References

- [1] S. Wagner, A. Pundt, Quasi-thermodynamic model on hydride formation in palladium-hydrogen thin films: impact of elastic and microstructural constraints, *Int. J. Hydrog. Energy* 41 (4) (2016) 2727–2738.
- [2] S. Wagner, T. Kramer, H. Uchida, P. Dobron, J. Cizek, A. Pundt, Mechanical stress and stress release channels in 10–350 nm palladium hydrogen thin films with different micro-structures, *Acta Mater.* 114 (2016) 116–125.
- [3] R. Schwarz, A. Khachaturyan, Thermodynamics of open two-phase systems with coherent interfaces, *Phys. Rev. Lett.* 74 (13) (1995) 2523.
- [4] A. Baldi, M. Gonzalez-Silveira, V. Palmisano, B. Dam, R. Griessen, Destabilization of the Mg-H system through elastic constraints, *Phys. Rev. Lett.* 102 (22) (2009) 226102.
- [5] M. Armand, J.-M. Tarascon, Building better batteries, *Nature* 451 (7179) (2008) 652–657.
- [6] J. Weissmuller, C. Lemier, On the size dependence of the critical point of nanoscale interstitial solid solutions, *Philos. Mag. Lett.* 80 (6) (2000) 411–418.

- [7] F. Larche, J.W. Cahn, The interactions of composition and stress in crystalline solids, *J. Res. Natl. Bur. Stand.* 89 (6) (1984) 467.
- [8] C. Lemier, J. Weissmüller, Grain boundary segregation, stress and stretch: effects on hydrogen absorption in nanocrystalline palladium, *Acta Mater.* 55 (4) (2007) 1241–1254.
- [9] S. Wagner, H. Uchida, V. Burlaka, M. Vlach, M. Vlcek, F. Lukac, J. Cizek, C. Baehz, A. Bell, A. Pundt, Achieving coherent phase transition in palladium–hydrogen thin films, *Scr. Mater.* 64 (10) (2011) 978–981.
- [10] V. Burlaka, S. Wagner, M. Hamm, A. Pundt, Suppression of phase transformation in Nb-H thin films below switchover thickness, *Nano Lett.* 16 (10) (2016) 6207–6212.
- [11] J. Eshelby, *The Continuum Theory of Lattice Defects*, *Solid State Physics*, vol. 3, Elsevier, 1956, pp. 79–144.
- [12] W. Nix, B. Clemens, Crystallite coalescence: a mechanism for intrinsic tensile stresses in thin films, *J. Mater. Res.* 14 (8) (1999) 3467–3473.
- [13] R. Gremaud, M. Gonzalez-Silveira, Y. Pivak, S. De Man, M. Slaman, H. Schreuders, B. Dam, R. Griessen, Hydrogenography of PdHx thin films: influence of H-induced stress relaxation processes, *Acta Mater.* 57 (4) (2009) 1209–1219.
- [14] S. Wagner, A. Pundt, Mechanical stress impact on thin Pd1-xFex film thermodynamic properties, *Appl. Phys. Lett.* 92 (5) (2008).
- [15] L. Mooij, B. Dam, Hysteresis and the role of nucleation and growth in the hydrogenation of Mg nanolayers, *Phys. Chem. Chem. Phys.* 15 (8) (2013) 2782–2792.
- [16] A. Baldi, L. Mooij, V. Palmisano, H. Schreuders, G. Krishnan, B.J. Kooi, B. Dam, R. Griessen, Elastic versus alloying effects in Mg-based hydride films, *Phys. Rev. Lett.* 121 (25) (2018) 255503.
- [17] N. Patelli, M. Calizzi, L. Pasquini, Interface enthalpy-entropy competition in nanoscale metal hydrides, *Inorganics* 6 (1) (2018) 13.
- [18] Y. Manassen, H. Realpe, D. Schweke, Dynamics of H in a thin Gd film: evidence of spinodal decomposition, *J. Phys. Chem. C* 123 (18) (2019) 11933–11938.
- [19] S. Wagner, P. Klose, V. Burlaka, K. Nörthemann, M. Hamm, A. Pundt, Structural phase transitions in niobium hydrogen thin films: mechanical stress, phase equilibria and critical temperatures, *ChemPhysChem* 20 (14) (2019) 1890–1904.
- [20] M. Hamm, V. Burlaka, S. Wagner, A. Pundt, Achieving reversibility of ultra-high mechanical stress by hydrogen loading of thin films, *Appl. Phys. Lett.* 106 (24) (2015).
- [21] A. Dyck, T. Böhlke, A. Pundt, S. Wagner, Phase transformation in the palladium hydrogen system: effects of boundary conditions on phase stabilities, *Scr. Mater.* 247 (2024) 116117.
- [22] K. Nörthemann, A. Pundt, Coherent-to-semi-coherent transition of precipitates in niobium-hydrogen thin films, *Phys. Rev. B* 78 (1) (2008) 014105.
- [23] G.G. Stoney, The tension of metallic films deposited by electrolysis, *Proc. R. Soc. Lond. Ser. A, Contain. Pap. Math. Phys. Character* 82 (553) (1909) 172–175.
- [24] M.E. Gurtin, E. Fried, L. Anand, *The Mechanics and Thermodynamics of Continua*, Cambridge University Press, 2010.
- [25] P. Rosakis, A. Rosakis, G. Ravichandran, J. Hodowany, A thermodynamic internal variable model for the partition of plastic work into heat and stored energy in metals, *J. Mech. Phys. Solids* 48 (3) (2000) 581–607.
- [26] R.v. Mises, *Mechanik der plastischen Formänderung von Kristallen*, *ZAMM-Journal of Applied Mathematics and Mechanics (Zeitschrift für Angewandte Mathematik und Mechanik)* 8 (3) (1928) 161–185.
- [27] A. Pundt, M. Suleiman, C. Bähz, M. Reetz, R. Kirchheim, N. Jisrawi, Hydrogen and Pd-clusters, *Mater. Sci. Eng. B* 108 (1–2) (2004) 19–23.
- [28] J.W. Gibbs, On the equilibrium of heterogeneous substances, *Trans. Conn. Acad. Arts Sci.* (1876) 108–248.
- [29] C.V. Di Leo, L. Anand, Hydrogen in metals: a coupled theory for species diffusion and large elastic–plastic deformations, *Int. J. Plast.* 43 (2013) 42–69.
- [30] A. Dyck, L. Groß, J. Keursten, L. Kehrer, T. Böhlke, Modeling and FE simulation of coupled water diffusion and viscoelasticity in relaxation tests of polyamide 6, *Contin. Mech. Thermodyn.* (2024) 1–19.
- [31] H. Peisl, Lattice strains due to hydrogen in metals, in: *Hydrogen in Metals I: Basic Properties*, 2005, pp. 53–74.
- [32] U. Laudahn, S. Fähler, H. Krebs, A. Pundt, M. Bicker, U. v. Hülsen, U. Geyer, R. Kirchheim, Determination of elastic constants in thin films using hydrogen loading, *Appl. Phys. Lett.* 74 (5) (1999) 647–649.
- [33] S. Wagner, M. Hamm, A. Pundt, Huge hydrogen-induced resistive switching in percolating palladium thin films, *Scr. Mater.* 69 (10) (2013) 756–759.